J Mater Sci (2007) 42:3936–3943
DOI 10.1007/s10853-006-0424-x

Synthesis and nonlinear optical properties of novel Y-type polyurethanes with high thermal stability of dipole alignment

Ju-Yeon Lee · Jin-Hyang Kim · Won-Taek Jung · Young Kum Park

Received: 18 March 2006 / Accepted: 8 May 2006 / Published online: 13 February 2007

Abstract 2,3-Di-(2′-hydroxyethoxy)benzylidenemalononitrile (**3**) was prepared and condensed with 2,4-toluenediisocyanate and 3,3′-dimethoxy-4,4′-biphenylenediisocyanate to yield novel Y-type polyurethanes **4–5** containing 2,3-dioxy benzylidenemalononitrile group as a nonlinear optical (NLO)-chromophore, which constituted parts of the polymer backbones. Polyurethanes **4–5** were soluble in common organic solvents such as acetone and *N,N*-dimethylformamide. They showed a thermal stability up to 270 °C in thermogravimetric analysis thermograms and the glass-transition temperatures (T_g) obtained from differential scanning calorimetry thermograms were around 116–135 °C. The second harmonic generation (SHG) coefficients (d_{33}) of poled polymer films at 106.4 mm^{-1} fundamental wavelength were around 9.07×10^{-19} C (2.72×10^{-9} esu). The dipole alignment exhibited high thermal stability up to 10 °C higher than T_g, and there was no SHG decay below 145 °C due to the partial main-chain character of the polymer structure, which was acceptable for nonlinear optical device applications.

Introduction

Organic nonlinear optical (NLO) materials have been extensively studied over the past decade because of their potential applications in the field of electro-optic devices [1–3]. Among the organic materials the NLO polymers are considered candidate materials, mainly because they offer many advantages such as mechanical endurance, light weight, chemical resistance, and good processability to form optical devices [4–7]. One of the current challenges is to design novel NLO polymers having optimized properties. In the developments of NLO polymers for electro-optic device applications, stabilization of electrically induced dipole alignment is important considerations. Two approaches to minimize the randomization have been proposed. One is to use a crosslinked system [8–13] and the other is to utilize polymers with a high glass transition temperature (T_g) polymers such as polyimides [14–22]. The polyurethane matrix forms extensive hydrogen bonding between urethane linkage and increases rigidity preventing the relaxation of induced dipoles. Polyurethanes with hemicyanine [23] and thiophene chromophore [24] in side chain showed an enhanced thermal stability of aligned dipoles. Polyurethanes with a NLO chromophore, whose dipole moment is aligned transverse to the main chain, showed large second-order nonlinearity with good thermal stability [25, 26]. Physically crosslinked systems via hydrogen bonds have the advantages such as homogenity and good processibility relative to chemically crosslinked systems, which suffer from significant optical loss and poor processability. In this work we have prepared novel Y-type polyurethanes containing the dioxybenzylidenemalononitrile groups as

---

J.-Y. Lee (✉) · J.-H. Kim · W.-T. Jung
Department of Chemistry, Institute of Functional Materials, Inje University, 607 Obang-dong, Gimhae 621-749, Seoul, Korea
e-mail: chemljy@inje.ac.kr

Y. K. Park
PDT Research Institute, School of Nano Engineering, Inje University, 607 Obang-dong, Gimhae 621-749, Seoul, Korea

NLO-chromophores. We selected 2,3-dioxy benzylidenemalononitrile groups as NLO-chromophores because they have a large dipole moment and are rather easy to synthesize. Furthermore, the 2,3-dioxybenzylidenemalononitrile groups constitute novel Y-type NLO polyurthanes (see Fig. 1c, [27]), in which the structure of NLO chromophore 2,3-dioxybenzylidenemalononitrile group is similar to the shape of letter "Y", and this Y-type NLO polyurethanes are not described in the literature. Thus we made a new type of NLO polyurethane, in which the pendant NLO-chromophores are part of the polymer backbones. These mid-type NLO polymers are expected to have the advantages of both main-chain and side-chain NLO polymers; stabilization of dipole alignment and good solubility. After confirming the structure of the resulting polymers, we investigated properties such as T_g, thermal stability, surface morphology, and second harmonic generation (SHG) activity (d_{33}). We now report the results of the initial phase of the work.

Experimental

Materials

The reagent-grade chemicals were purchased from Aldrich and purified by either distillation or recrystallization before use. 2-Chloroethyl vinyl ether and 2,3-dihydroxybenzaldehyde were used as received. 2,4-Toluenediisocyanate (TDI) was purified by distillation under reduced pressure. 3,3′-Dimethoxy-4,4′-biphenylenediisocyanate (DMBPI) was recrystallized from ethyl acetate. Piperidine was dried with calcium hydride and fractionally distilled. *N,N*-Dimethylformamide (DMF) was purified by drying with anhydrous calcium sulfate, followed by distillation under reduced pressure.

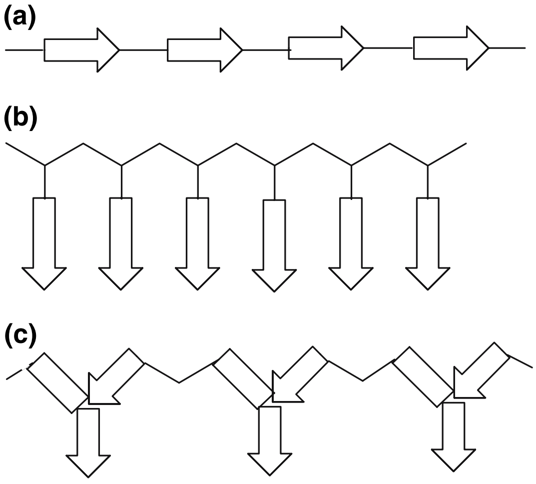

Fig. 1 (**a**) Main-chain NLO polymers, (**b**) side-chain NLO polymers, and (**c**) Y-type NLO polymers

Measurements

IR spectra were taken on a Shimadzu FT IR-8201PC infrared spectrophotometer. ^{1}H NMR spectra were obtained on a Varian 300 MHz NMR spectrometer. UV–VIS absorption spectra were measured on a Shimadzu UV-3100S spectrophotometer. Elemental analyses were performed using a Perkin–Elmer 2400 CHN elemental analyzer. The glass transition temperatures (T_g) were measured on a TA 2920 differential scanning calorimeter in a nitrogen atmosphere. DuPont 951 thermogravimetric analyzer with a heating rate of 10 °C/min up to 800 °C was used for the thermal degradation study of polymers under nitrogen. The number average molecular weight (M_n) and weight average molecular weight (M_w) of the polymers were estimated by gel permeation chromatography (GPC) (columns styragel HR5E4E; solvent THF). Atomic force microscopy (AFM) images were recorded with a Park Science Instrument Autoprobe CP, operated in a contact mode, which measures topography. Melting points were measured in Buchi 530 melting point apparatus and are corrected. Viscosity values were obtained by using a Cannon-Fenske viscometer.

Film preparation and SHG measurements

The polymer film was prepared from a 10% by weight polymer solution in DMF deposited on an indium–tin oxide (ITO) covered glass. Prior to film casting, the polymer solution was filtered through 0.45 μm Teflon membrane filter. The film was spin cast at room temperature at a range from 1,000 to 1,200 rpm. The films were dried for 12 h under vacuum at 60 °C. The alignment of the NLO-chromophore of the polymers was carried out by corona poling method. The poling was performed in a wire-to-plane geometry under in situ conditions. The discharging wire to plane distance was 10 mm. As the temperature was raised gradually to 5–10 °C higher than T_g, 6.5 kV of corona voltage was applied and kept that temperature for 30 min. The films were cooled to room temperature in the presence of the electric field. Finally, the electric field was removed. The refractive index of the sample was measured by the optical transmission technique [28]. The transmittance of thin film includes on the information of the thickness, refractive index and extinction coefficient of that. Thus, we can determine these parameters by analyzing the transmittance. Second harmonic generation (SHG) measurement was carried out 1 day after poling. A continuum PY61 mode-locked Nd:YAG laser (λ = 1,064 nm) with pulse width of 40 ps and repetition rate of 10 Hz was used as the fundamental light source and Y-cut quartz was used as reference. A beam splitter and a photodiode were used to compensate for the intensity fluctuations of the fundamental beam (1,064 nm). The polarity of the fundamental laser beam was adjusted using a half-wave plate before it hit the sample. The electric field vector of the incident beam was either parallel (*p*-polarization) or perpendicular (*s*-polarization) to the plane of incidence. Only the *p*-polarized SH beam was made to enter a photomultiplier tube (PMT) by using a prism and a SH pass filter. An analyzer was used to confirm the polarization direction of the SH signal. A poled polymer film was mounted on the rotator coupled to a step motor. The output signals from the photodiode and PMT were detected as a function of an incident angle. A 3-mm-thick Y-cut quartz crystal (a piece of quartz plate whose plane is perpendicular to the crystalline *y*-axis and the thickness of the plate is 3 mm and d_{11} = 0.3 pm/V) was used as a reference for determining the relative intensities of the SH signals generated from the samples. The Maker Fringe pattern was obtained from measuring the SHG signal at 0.5° intervals using a rotation stage. SHG coefficients (d_{33}) were derived from the analysis of measured Maker-fringes [29–32].

2,3-Di-(2′-vinyloxyethoxy)benzaldehyde (**1**)

2,3-Dihydroxybenzaldehyde (13.8 g, 0.10 mol), anhydrous potassium carbonate (36 g, 0.36 mol), and 2-chloroethyl vinyl ether (26.6 g, 0.25 mol) were dissolved in 2×10^{-4} m^3 of dry DMF under nitrogen. The mixture was refluxed in an oil bath kept at 100 °C for 40 h under nitrogen. The resulting solution was cooled to room temperature, diluted with 3×10^{-4} m^3 of water, and extracted with 3×10^{-4} m^3 of diethyl ether three times. The organic layer was washed with saturated aqueous sodium chloride solution, and dried with anhydrous magnesium sulfate. Rotary evaporation of diethyl ether gave crude product, which was recrystallized from 1-butanol yielded 24.5 g (88% yield) of pure product **1**. Mp = 48–50 °C. ^{1}H NMR ($CDCl_3$) δ 3.95–4.47 (m, 12H, 2 CH_2= 2 –O–CH_2–CH_2–O–), 6.44–6.57 (m, 2H, 2 =CH–O–), 7.09–7.19 (m, 2H, aromatic), 7.42–7.48 (m, 1H, aromatic), 10.48 (s, 1H, –CHO). IR (KBr) 3098, 3076 (w, =C–H), 2953, 2883 (s, C–H), 1682 (vs, C=O), 1618 (vs, C=C) cm^{-1}.

2,3-Di-(2′-vinyloxyethoxy) benzylidenemalononitrile (**2**)

Piperidine (0.13 g, 1.5 mmol) was added to a solution of 2,3-di-(2′-vinyloxyethoxy)benzaldehyde **1** (8.35 g, 30 mmol) and malononitrile (2.18 g, 33 mmol) in 1.7×10^{-4} m^3 of 1-butanol with stirring at 0 °C under nitrogen. After stirring for 4 h at 0 °C, the reaction mixture was cooled to –10 °C for crystallization. The product was filtered and washed successively with cold 1-butanol (8×10^{-5} m^3), water (3×10^{-5} m^3), and cold 1-butanol (2×10^{-5} m^3). The obtained pale yellow product was recrystallized from 1-butanol to give 8.11 g (83% yield) of **2**. Mp = 60–62 °C. ^{1}H NMR ($CDCl_3$) δ 3.90–4.42 (m, 12H, 2 CH_2=, 2 –O–CH_2–CH_2–O–), 6.45–6.57 (m, 2H, 2 =CH–O–), 7.13–7.20 (d, 2H, aromatic), 7.80–7.87 (t, 1H, aromatic), 8.47 (s, 1H, Ph–CH=). IR (KBr) 3116, 3059 (w, =C–H), 2941, 2885 (m, C–H), 2233 (s, CN), 1618, 1572 (vs, C=C) cm^{-1}. Anal. Calcd. for $C_{18}H_{18}N_2O_4$: C, 66.25; H, 5.56; N, 8.58. Found: C, 66.34; H, 5.63; N, 8.48.

2,3-Di-(2′-hydroxyethoxy) benzylidenemalononitrile (**3**)

Aqueous hydrochloric acid (1.5 M, 3×10^{-5} m^3) was slowly added to a solution of 2,3-di-(2′-vinyloxyethoxy)benzylidenemalononitrile (**2**) (8.48 g, 0.026 mol) in 6×10^{-5} m^3 of dry THF with stirring under nitrogen at 0 °C. The mixture was stirred at 80 °C for 8 h under nitrogen. The resulting solution was extracted with diethyl ether (8×10^{-5} m^3) three times. The organic layer was washed successively with saturated sodium chloride, sodium hydrogen carbonate, and water, followed by drying with anhydrous magnesium sulfate. Rotary evaporation of diethyl ether gave crude product. The obtained pale yellow product was recrystallized from ethyl acetate to give 5.85 g (82% yield) of **3**. Mp: 116–118 °C. ^{1}H NMR (acetone-d_6) δ 3.75–3.96 (m, 4H, 2 –CH_2–OH), 4.12–4.25 (m, 4H, 2 –O–CH_2–), 4.26–4.34 (t, 2H, –OH), 7.21–7.29 (t, 1H, aromatic), 7.37–7.44 (d, 1H, aromatic), 7.72–7.78 (d, 1H, aromatic), 8.75 (s, 1H, –Ph–CH=). IR (KBr) 3360, 3256 (s, O–H), 3044 (w, =C–H), 2941 (m, C–H), 2222 (m, CN), 1572 (vs, C=C) cm^{-1}. Anal. Calcd. for $C_{14}H_{14}N_2O_4$: C, 61.31; H, 5.14; N, 10.21. Found: C, 61.38; H, 5.23; N, 10.12.

Synthesis of polyurethanes **4–5**

A representative polycondensation reaction procedure (the case of **4**) was as follows: 2,4-Toluenediisocynate (1.74 g, 0.01 mol) was added slowly to a solution of 2.74 g of diol **3** (0.01 mol) in 2.5×10^{-5} m^3 of anhydrous DMF. The resulting solution was degassed by a freeze–thaw process under vacuum and placed in an oil bath kept at 80 °C. After heating 12 h with stirring the polymerization tube was opened and the viscous polymer solution was poured into 4×10^{-4} m^3 of cold water. The precipitated polymer was collected and reprecipitated from DMSO into methanol. The polymer was further purified by extraction in a Soxhlet extractor with diethyl ether and dried under vacuum to give 3.95 g (88% yield) of polymer **4**: $\eta_{inh} = 2.8 \times 10^{-5}$ m^3/g (c, 5×10^3 g/m^3 in DMSO at 25 °C). ^1H NMR (DMSO-d_6) δ 2.08 (s, 3H, $-CH_3$), 4.25–4.48 (t, 8H, 2 $-O-CH_2-CH_2-O-$), 6.97–7.65 (m, 6H, aromatic), 8.49 (s, 1H, Ph–CH=), 8.77–8.91 (t, 1H, N–H), 9.53–9.66 (d, 1H, N–H). IR (KBr) 3360 (s, N–H), 2964 (m, C–H), 2233 (m, CN), 1722 (vs, C=O), 1595 (s, C=C) cm^{-1}. Anal. Calcd. for $(C_{23}H_{20}N_4O_6)_n$: C, 61.60; H, 4.50; N, 12.49. Found: C, 61.52; H, 4.61; N, 12.57. Polymer **5**: $\eta_{inh} = 2.6 \times 10^{-5}$ m^3/g (c, 5×10^3 g/m^3 in DMSO at 25 °C). ^1H NMR (DMSO-d_6) δ 3.86 (s, 6H, 2 $-OCH_3$), 4.27–4.53 (t, 8H, 2 $-O-CH_2-CH_2-O-$), 7.13–7.76 (m, 7H, aromatic), 8.17–8.56 (t, 3H, aromatic), 8.59 (s, 1H, N–H), 9.01 (s, 1H, N–H). IR (KBr) 3420 (m, N–H), 2953 (m, C–H), 2233 (m, CN), 1733 (s, C=O), 1589 (s, C=C) cm^{-1}. Anal. Calcd. for $(C_{30}H_{26}N_4O_8)_n$: C, 63.15; H, 4.59; N, 9.82. Found: C, 63.26; H, 4.66; N, 9.86.

Results and discussion

Synthesis and characterization of polymers 4–5

2,3-Di-(2′-vinyloxyethoxy)benzaldehyde (**1**) was prepared by the reaction of 2-chloroethyl vinyl ether with 2,3-dihydroxybenaldehyde. 2,3-Di-(2′-vinyloxyethoxy) benzylidenemalononitrile (**2**) was prepared by the condensation reaction of **1** with malononitrile [33]. Diol **3** was obtained by acid-catalyzed hydrolysis of compound **2**. The synthetic route for compound **3** is presented in Scheme 1. Polymers **4** and **5** were prepared by the polyaddition reaction between a diol **3** and 2,4-toluenediisocyanate (TDI) and 3,3′-dimethoxy-4,4′-biphenylenediisocyanate in a dry DMF solvent (see Scheme 2). Polymerization results are summarized in Table 1. The polymerization yield was 82–90%. The chemical structures of the compounds were identified by ^1H NMR, IR spectra and elemental analysis. Elemental analysis results fit the polymer structures. ^1H NMR spectra of the polymers showed a signal broadening due to polymerization, but the chemical shifts are consistent with the proposed polymer structures. The signal at 8.59–9.66 ppm assigned to the amine proton indicates the formation of urethane linkage. The IR spectra of the same polymer samples also show a strong carbonyl peak near 172.2 mm^{-1} indicating the presence of urethane bond. The number average molecular weights (M_n) of the polymers were determined to be 21,300 ($M_w/M_n = 1.86$) for polymer **4**. Polydispersities were in the range of 1.97–2.13. The polymers **4–5** were soluble in common solvents such as acetone, DMF, and DMSO, but were not soluble in methanol and diethyl ether. The inherent viscosity values were in the range of 2.5×10^{-5}–2.8×10^{-5} m^3/g. Polymers **4–5** showed strong absorption near 320 nm by the NLO-chromophore dioxybenzylidenemalononitrile group. The striking feature of this polymerization system is that it gives unprecedented T-type NLO polymers, in which the pendant NLO chromophores are part of the polymer backbones. These mid-type NLO polymers are expected to have the advantages of both main-chain and side-chain NLO polymers. Thus, we obtained a new type of NLO polyurethane with side-chain and main-chain characteristics. We now have well defined Y-type polyurethanes (**4–5**) and investigate their properties.

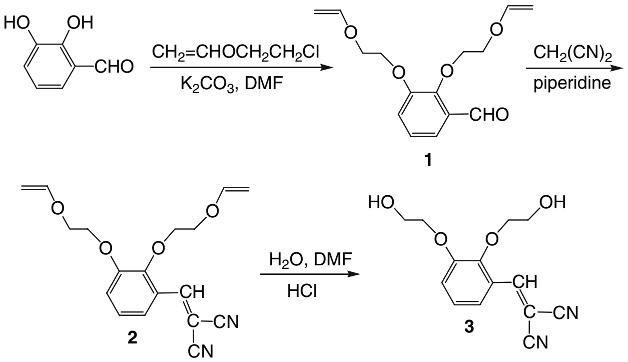

Scheme 1 Synthesis of diol **3**

Thermal properties of the polymers

The thermal behavior of the polymers was investigated by thermogravimetric analysis (TGA) and differential scanning calorimeter (DSC) to determine the thermal degradation pattern and glass transition temperature (T_g). The results are summarized in Table 2. In Figs. 2 and 3, TGA and DSC thermograms of the polymers **4–5** are presented, respectively. Polymers **4–5** showed a thermal stability up to 270 °C according to their TGA thermograms. The initial weight loss in the polymers begins at 248–275 °C. Polymer **5** showed a higher initial degradation temperature. The T_g values of the polymers **4–5** measured by DSC were around 116–135 °C. Polymer **5** exhibited a higher T_g value than **4** and can probably be attributed to the rigidity of the polymer backbone containing biphenyl group.

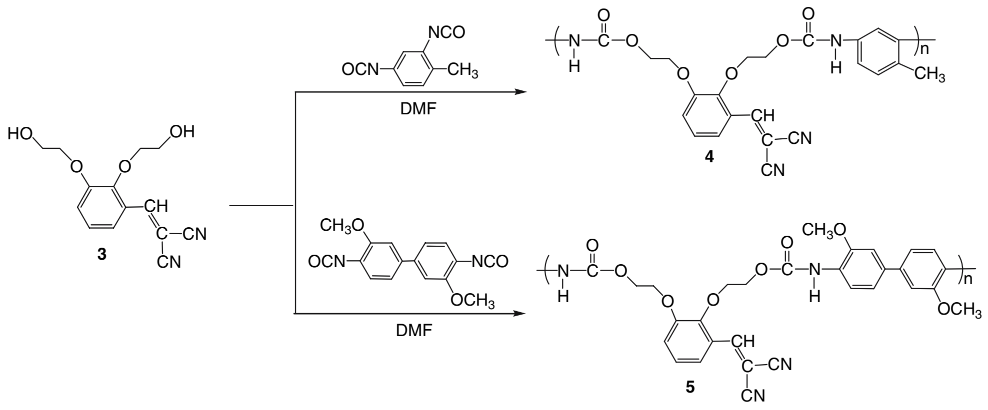

Scheme 2 Synthesis of polymers **4–5**

Table 1 Polymerization of **3**[a] with TDI[b] and DMBPI[c] in DMF

Monomer	Monomer/sovent (mol/m^3)	Diol **3** to RNCO (mol/mol)	Time (h)	Yield (%)	η^{d}_{inh} (10^{-5} m^3/g)	M_n^e	M_w^e	PD[f]
3, TDI	400	1.0	10	86	2.6	21,300	39,600	1.86
3, TDI	800	1.0	12	88	2.8	18,500	36,700	1.98
3, DMBPI	400	1.0	10	85	2.5	16,900	34,400	2.04
3, DMBPI	800	1.0	12	86	2.6	19,300	37,600	1.95

[a] **3** = 2,3-Di-(2′-hydroxyethoxy)benzylidenemalononitrile

[b] TDI = 2,4-Toluendiisocyanate

[c] DMBPI = 3,3′-Dimethoxy-4,4′-biphenylenediisocyanate

[d] Inherent viscosity of polymer: concentration of 5×10^3 g/m^3 in DMSO at 25 °C

[e] Measured by GPC in THF using polystyrene standard

[f] PD = Polydispersity

Table 2 Thermal properties of polymers **4–5**

Polymer	T_g^a (°C)	Degradation temp (°C)[b]				Residue at 800 °C (%)[b]
		Initial-loss	5%-loss	20%-loss	40%-loss	
4	116	248	276	297	332	14.7
5	135	275	289	329	359	25.5

[a] Determined from DSC curves measured on a TA 2920 differential scanning calorimeter with a heating rate of 10 °C/min under nitrogen atmosphere

[b] Determined from TGA curves measured on a DuPont 951 thermogravimetric analyzer with a heating rate of 10 °C/min under nitrogen atmosphere

Nonlinear optical properties of the polymers

The NLO properties of polymers were studied by the SHG method. To induce noncentrosymmetric polar order, the spin-coated polymer films were corona-poled. As the temperature was raised gradually to 5–10 °C higher than T_g, 6.5 kV of corona voltage was applied and kept that temperature for 30 min. The poling was confirmed by UV–VIS spectra. Figure 4 shows the UV–VIS absorption spectra of the polymer sample **4** before and after the poling. Polymers **4–5** showed strong absorption near 320 nm by the NLO-chromophore 2,3-dioxybenzylidenemalononitrile group. After the electric poling, the dipole moments of the NLO-chromophores were aligned and UV–VIS spectrum of polymer **4** exhibited a decrease in absorption due to birefringence. From the absorbance change, the order parameter of the poled film could be estimated, which is related to the poling efficiency. The estimated order parameter value Φ was found to have a value of 0.12 for polymer **4** ($\Phi = 1 - A_1/A_0$, where A_0 and A_1 are the absorbances of the polymer film before and after poling, respectively). For the purpose of investigating surface morphology of polymer films, domain

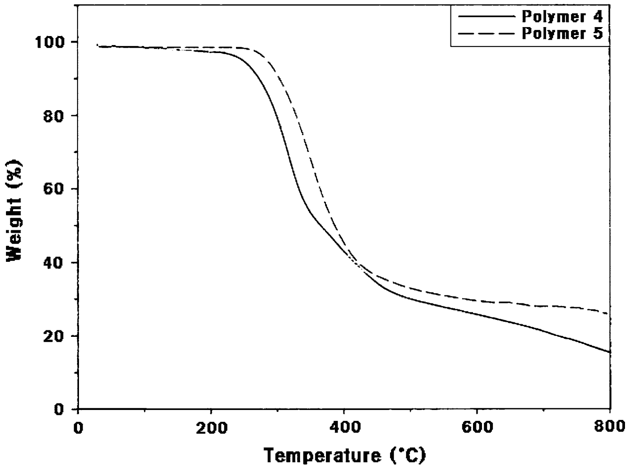

Fig. 2 TGA thermograms of polymers **4**–**5** at a heating rate of 10 °C/min under nitrogen

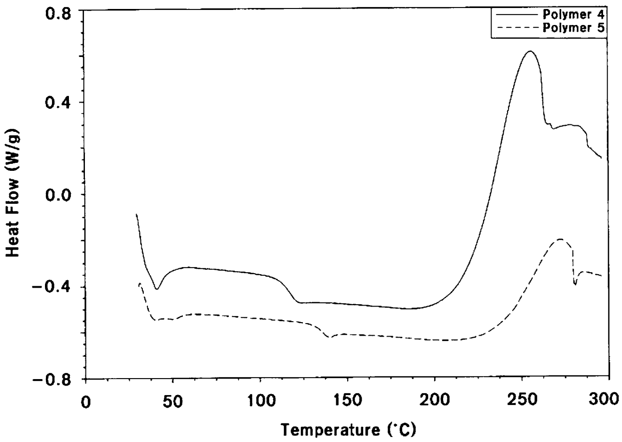

Fig. 3 DSC thermograms of polymers **4**–**5** at a heating rate of 10 °C/min under nitrogen

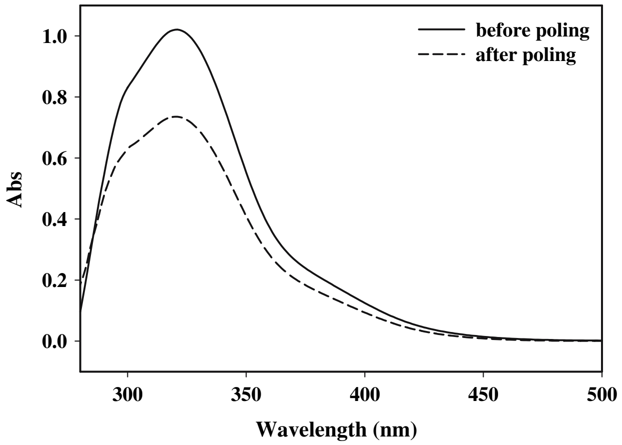

Fig. 4 UV–VIS absorption spectra of a film of polymer **4** before and after poling

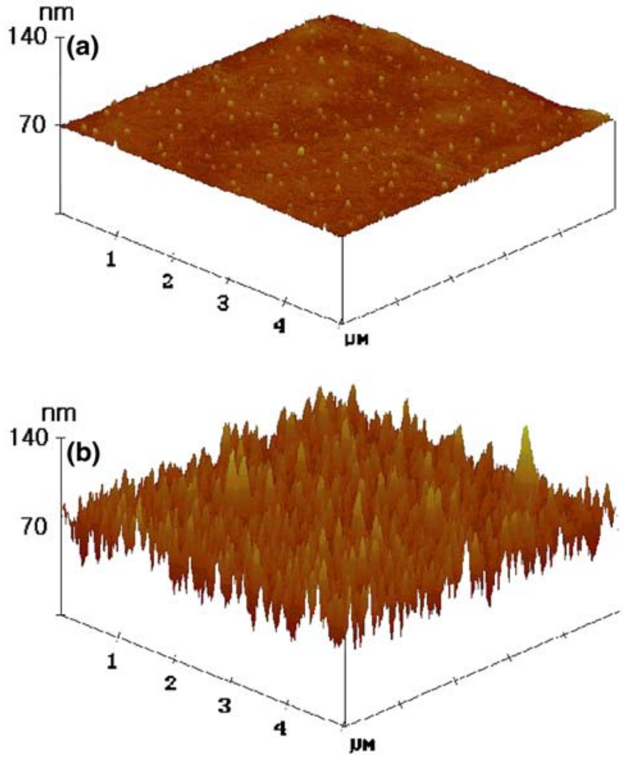

Fig. 5 AFM images of spin-coated film of polymer **4**: (**a**) before corona-poling; (**b**) after corona-poling

structures of NLO-chromophores for the thin-film samples were obtained using atomic force microscopy (AFM). Figure 5 shows AFM scans of the spin-coated film before and after poling for polymer **5**. AFM images show that the surface of the film sample is extremely flat and clean before poling (see Fig. 5a). However, this good quality film was dramatically changed after poling, resulting in numerous hills and valleys in the surface structure, which means that the NLO-chromophores are aligned the poling direction as shown in Fig. 5b. The refractive index of the sample was measured by the optical transmission technique [28]. The transmittance of thin film includes the information of the thickness, refractive index and extinction coefficient of that. Thus, we can determine those parameters by analyzing the transmittance. SHG measurements were performed at a fundamental wavelength of 1,064 nm using a mode locked Nd-YAG laser [29–32]. In order to determine the microscopic second-order susceptibility of the polymers, the angular SHG dependence was recorded. Figure 6 shows the angular dependence of SHG signal in a poled polymer **5**. The SHG values were compared with those obtained from a Y-cut quartz plate. To calculate the d_{31} and d_{33} values, both *s*-polarized and *p*-polarized IR laser were directed to the samples and recorded.

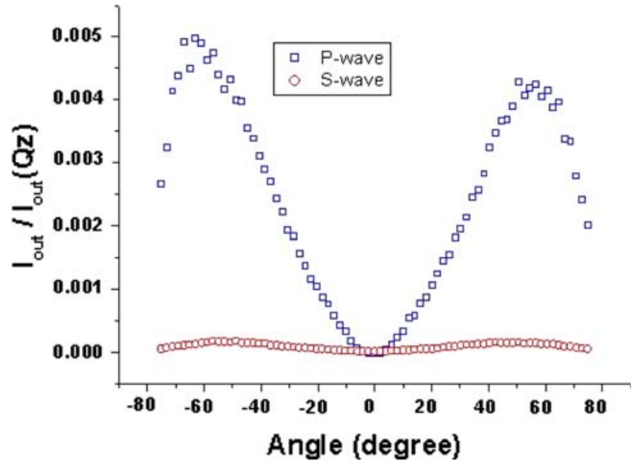

Fig. 6 Angular dependence of SHG signal in a poled film of polymer **5**

Nonlinear optical properties of polymers **4–5** are summarized in Table 3. SHG coefficients (d_{33}) were derived from the analysis of measured Maker-fringes with Pascal fitting program according to the literature procedure [32]. The values of d_{31} and d_{33} for polymer **4** were 3.21×10^{-19} and 9.07×10^{-19} C, respectively. Since the second harmonic wavelength was at 532 nm, which is not in the absorptive region of the resulting polyurethane, there was not resonant contribution to this d_{33} value. In the isotropic model, the ratio of d_{33}/d_{31} is predicted to be about 3. Our d_{33}/d_{31} value of 2.8 is in good agreement with the predicted value. To evaluate the high-temperature stability of the polymers, we studied the temporal stability of the SHG signal. In Fig. 7, we present the dynamic thermal stability study of the NLO activity of the film **5**. To investigate the real time NLO decay of the SHG signal of the poled polymer films as a function of temperature, in situ SHG measurements were performed at a heating rate of 10 °C/min from 30 to 180 °C. The polymer film exhibited a greater thermal stability even at 10 °C higher than T_g and no significant SHG decay was observed below 145 °C. In general, side-chain NLO polymers loose thermal stability of dipole alignment below T_g. Stabilization of dipole alignment is a characteristic of main chain NLO polymers. The exceptional high thermal stability of second harmonic generation of polymers **4–5** was due to the stabilization of dipole alignment of NLO chromophore, which stemmed from the partial main chain character of the polymer structure. The polymers also showed good long-term thermal stability of d_{33} except for the small activity loss within a few days after poling, which are acceptable for NLO device applications. Thus, we obtained a new type of NLO polyurethane having the advantages of both main-chain and side-chain NLO polymers: stabilization of dipole alignment and good solubility.

Conclusions

We synthesized novel Y-type polyurethanes **4–5** with pendant NLO chromophores, which were parts of the

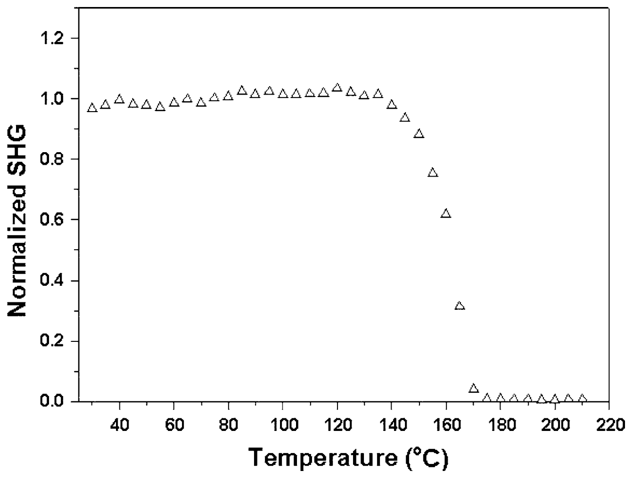

Fig. 7 Normalized SHG signal of polymer **5** as a function of temperature at a heating rate of 10 °C/min

Table 3 Nonlinear optical properties of polymers **4–5**

Polymer	λ^{a}_{max} (nm)	d^{b}_{33} (C)	Φ^{c}	Film thickness[d] (μm)	d^{b}_{31} (C)	n
4	321	$(9.07 \pm 0.40) \times 10^{-19}$	0.28	0.52	$(3.21 \pm 0.15) \times 10^{-19}$	$n_1 = 1.58$ $n_2 = 1.65$
5	318	$(9.94 \pm 0.46) \times 10^{-19}$	0.33	0.50	$(3.54 \pm 0.18) \times 10^{-9}$	$n_1 = 1.56$ $n_2 = 1.63$

[a] Polymer film after corona poling

[b] SHG coefficients (d_{33}) were derived from the analysis of measured Maker-fringes [32]

[c] Order parameter $\Phi = 1 - A_1/A_0$, where A_0 and A_1 are the absorbances of the polymer film before and after corona poling, respectively

[d] Film thickness was determined by the optical transmission technique [28]

polymer main chains. These mid-type NLO polyurethanes are soluble in common organic solvents. The resulting polymers **4–5** showed a thermal stability up to 270 °C from TGA thermograms with T_g values in the range of 116–135 °C. The SHG coefficients (d_{33}) of corona-poled polymer films were 9.07×10^{-19} C (2.72×10^{-9} esu). The striking feature of these polymers is that they exhibit SHG stability up to 10 °C higher than T_g and no SHG decay was observed below 145 °C. This exceptional high thermal stability of optical nonlinearity stemmed from the stabilization of dipole alignment of the NLO-chromophore, which constituted a part of the polymer backbone, which was acceptable for NLO device applications. We are now in the process of extending the polymerization system to the synthesis of other type of NLO polymers and the results will be reported elsewhere.

Acknowledgement This work was supported by Korea Institute of Industrial Technology Evaluation and Planning (Regional Industrial Technology Development Program 11016015).

References

1. Williams D (1988) In: Bowden MJ, Turner SR (eds) Electronic and photonic applications of polymers. American Chemical Society, Washington, DC, pp 297–330
2. Prasad PN (1988) In: Preasad PN, Ulrich DR (eds) Nonlinear optical and elrctroactive polymers. Plenum Press, New York, pp 41–67
3. Thackara JI, Lipscomb GF, Lytel RS, Ticknor AJ (1988) In: Heeger AJ, Orenstein J, Ulrich DR (eds) Nonlinear optical properties of polymers. Materials Research Society, Pittsburgh, pp 19–27
4. Burland DM, Miller RD, Walsh C (1994) Chem Rev 94:31
5. Dalton LR, Harper AW, Ghosen R, Steniner WH, Ziari M, Fetterman H, Shi Y, Mustacich RV, Jen AKY, Shea KJ (1995) Chem Mater 7:1060
6. Dalton DR, Harper AW, Ghosen R, Laquindanum J, Liang Z, Hubble A, Xu C (1995) Adv Mater 7:519
7. Marks TJ, Ratner MA (1995) Angew Chem Int Ed Engl 34:155
8. Chen M, Yu L, Dalton LR, Shi Y, Steier WH (1992) Macromolecules 25:4032
9. Xu C, Wu B, Dalton LR, Shi Y, Ranon PM, Steier WH (1992) Macromolecules 25:6714
10. Boogers JAF, Klaase PTA, Vlieger JJD, Tinnemans AHA (1994) Macromolecules 27:205
11. Park CK, Zieba CF, Zhao CF, Swedek B, Wijekoon WMKP, Prasad PN (1995) Macromolecules 28:3713
12. Tsutumi N, Yoshizaki S, Sakai W, Kiyotsukuri T (1995) Macromolecules 28:6442
13. Han KS, Park SK, Shim SY, Jahng WS, Kim NJ (1998) Bull Korean Chem Soc 19:1165
14. Jeng RJ, Chen YM, Jain AK, Kumar J, Tripathy SK (1992) Chem Mater 4:1141
15. Becker MW, Sapochak LS, Ghosen R, Dalton LR (1994) Chem Mater 6:104
16. Pretre P, Kaatz P, Bohren A, Gunter P, Zysset B, Ahlheim M, Stahelin M, Lehr F (1994) Macromolecules 27:5476
17. Yu D, Gharavi A, Yu L (1995) Macromolecules 28:784
18. Miller RD, Burland DM, Jurich M, Lee VY, Moylan CR, Thackara JI, Twieg RJ, Verbiest T, Volksen W (1995) Macromolecules 28:4970
19. Yu D, Gharavi A, Yu L (1995) J Am Chem Soc 117:11680
20. Yu D, Gharavi A, Yu L (1996) Macromolecules 29:6139
21. Saadeh H, Gharavi A, Yu D, Yu L (1997) Macromolecules 30:5403
22. Tsutsumi N, Morishima M, Sakai W (1998) Macromolecules 31:7764
23. Moon KJ, Shim HK, Lee KS, Zieba J, Prasad PN (1996) Macromolecules 29:861
24. Woo HY, Lee KS, Shim HK (2000) Polym J 32:8
25. Tsutumi N, Matsumoto O, Sakai W, Kiyotsukuri T (1996) Macromolecules 29:592
26. Tsutumi N, Matsumoto O, Saki W (1997) Macromolecules 30:4584
27. In Fig. 1(c), the double arrow means that 2-oxy electron-releasing group is conjugated with electron-withdrawing benzylidenemalononitrile group
28. Cisneros JI (1998) Appl Opt 37:5262
29. Maker PD, Terhune RW, Nisenoff M, Savage CM (1962) Phys Rev Lett 8:21
30. Jephagnon J, Kurtz SK (1970) J Appl Phys 40:1667
31. Singer DD, Sohn JE, Lalama SJ (1986) Appl Phys Lett 49:248
32. Herman WN, Hayden LM (1995) J Opt Soc Am B 12:416
33. Corson BB, Stoughton RS (1928) J Am Chem Soc 50:2825